Archives of Microbiology (2024) 206:267
https://doi.org/10.1007/s00203-024-03992-8

ORIGINAL PAPER

Exploring the evolutionary and pathogenic role of *Acinetobacter baumannii* biofilm-associated protein (Bap) through *in silico* structural modeling

Kirti Upmanyu[1,2] · Rakesh Kumar[1] · Qazi Mohd Rizwanul Haque[2] · Ruchi Singh[1]

Received: 5 March 2024 / Revised: 24 April 2024 / Accepted: 3 May 2024 / Published online: 18 May 2024

Abstract

Acinetobacter species encode for extracellularly secreted Biofilm-associated protein (Bap), a multi-domain protein with variable molecular weights reaching several hundred kilodaltons. Bap is crucial for the development of multi-dimensional structures of mature biofilms. In our investigation, we analyzed 7338 sequences of *A. baumannii* from the NCBI database and found that Bap or Bap-like protein (BLP) was present in 6422 (87.52%) isolates. Further classification revealed that 12.12% carried Type-1 Bap, 68.44% had Type-2, 6.91% had Type-3, 0.05% had Type-6 or SDF-Type, and 12.51% lacked Bap or BLP. The majority of isolates with Type-1, Type-2, and Type-3 Bap belonged to ST1, ST2, and ST25, respectively. Phylogenetic analysis suggested that Type-1 Bap is the most ancient, while Type-3 and SDF-Type have evolved recently. Studying the interaction of predicted Bap structures with human CEACAM-1 and PIgR showed that Bap with its BIg13 and BIg6 domains interact with the N-terminal domain of CEACAM-1, involving Arg^{43} and Glu^{40}, involved in CEACAM-1 dimerization. Also, we found that recently evolved Type-3 and SDF-Type Bap showed greater interaction with CEACAM-1 and PIgR. It can be asserted that the evolution of Bap has conferred enhanced virulence characteristics to *A. baumannii* with increased interaction with CEACAM-1 and PIgR. Using *in silico* approaches, this study explores the evolutionary, physicochemical, and structural features of *A. baumannii* Bap and unravels its crucial role in mediating interaction with human CEACAM-1 and PIgR through detailed structure modelling. These findings advance our understanding of *A. baumannii* Bap and highlight its role in pathogenesis.

Keywords Biofilm · Virulence · Pathogenesis · *A. Baumannii* · Biofilm associated protein (Bap) · Host pathogen interaction · CEACAM-1 · PIgR

Introduction

Acinetobacter baumannii, a Gram-negative coccobacillus, has emerged as an aggressive pathogen due to its ability to adapt resistance against various antibiotics rapidly and hence declared as a priority pathogen by WHO (Howard et al. 2012; Jung et al. 2017). Its ability to persist in the hospital environment encourages nosocomial infections, including ventilator-associated pneumonia, meningitis, bacteremia, urinary tract infection, and wound infections in immune-compromised patients (Greene et al. 2016a, b; Wong et al. 2017; Chapartegui-González et al. 2018). Biofilm formation by *A. baumannii* is a multifactorial complex process comprising initial adhesion by *csuABCDE* operon encoded chaperon usher (csu) pili and outer membrane protein A (OmpA); further maturation is facilitated by secretion of matrix components such as Biofilm-associated protein (Bap), and polysaccharides like poly N-acetyl glucosamine and alginate encoded by *pgaABCD* operon and *algC*, respectively (Gedefie et al. 2021). Among the *A. baumannii* population, these factors are reported to be conserved among isolates belonging to different clonal complexes; however,

Communicated by Yusuf Akhter.

✉ Ruchi Singh
ruchisp@gmail.com; ruchisingh.nip@gov.in

[1] ICMR-National Institute of Pathology, Safdarjung Hospital Campus, New Delhi 110029, India

[2] Department of Biosciences, Jamia Millia Islamia, New Delhi, India

heterogeneity persists in the genes encoding for OmpA and Bap (Viale and Evans 2020; De Gregorio et al. 2015). Bap, a hydrophobic cell surface protein, plays a crucial role in the adhesion of *A. baumannii* on human cells and medically relevant substances such as polystyrene, polypropylene, and titanium (Brossard and Campagnari 2012; Goh et al. 2013).

A. baumannii encodes for large multi-domain Bap with varying molecular weight of up to 879.60 kDa, secreted extracellularly and was identified as a homolog of Bap produced by *Staphylococcus aureus* (Loehfelm et al. 2008). In *A. baumannii* strain 307 − 0294, Bap was verified to facilitate the formation of multi-dimensional structures and water channels within biofilms, leading to mature biofilm. Conversely, the multi-domain mutant *A. baumannii* strain 307 − 0294 failed to produce mature biofilms and remained in a single layer, indicating its role in biofilm maturation rather than the initial stage of adherence (Loehfelm et al. 2008; Brossard and Campagnari 2012).

Bap consists of tandemly arranged repeated domains. The first half comprises A to C modules arranged in a multi-domain fashion. The second half comprises 28 direct tandem repeats of module D. Each module belongs to an immunoglobulin-like fold superfamily (Loehfelm et al. 2008). A previous study has shown that genome sequences of many *A. baumannii* isolates available in the National Center for Biotechnology Information (NCBI) database harbor mutations within the Bap gene, resulting in the production of disrupted Bap; this might be attributed to the repetitive regions of this gene, which may hinder accurate assembly (Goh et al. 2013). Despite the conservation of the majority of components involved in biofilm formation, the ability of *A. baumannii* to form biofilms varies within its population. This variation in phenotype variation may be attributed to various extrinsic and intrinsic factors including the genomic composition that describes the clonal complexity of the strain (Eze et al. 2018). Variations in the number and type of tandem repeats comprising Bap have been observed. Besides clonal complexity, variations in number and type of tandem repeats comprising Bap have been observed. The different Bap variants are categorized into four types based on their unique Ig-like domains (Loehfelm et al. 2008; De Gregorio et al. 2015).

It has been now recognized that different strains of *A. baumannii* elicit different immune responses in mice (De Breij et al. 2012; Kale et al. 2017; Morris et al. 2019). A study previously demonstrated that *A. baumannii* AB5075 interacts with carcinoembryonic antigen-related cell adhesion molecules (CEACAM) -1, -5, and − 6 present on the surface A549 cells, leading to the internalization of *A. baumannii* in a vacuole bound by the cellular membrane (Ambrosi et al. 2020). CEACAMs are expressed as transmembrane receptors on the surface of leukocytes, epithelial cells, and endothelial cells of blood vessels and play a vital role in adhesion, cell cycle regulation, insulin action, angiogenesis, and cancer (Singer et al. 2002; Öbrink 1997; Hammarström 1999; Bamberger et al. 2000; Najjar 2002). The role of adhesins and outer membrane proteins in binding to CEACAMs has been found in various bacterial pathogens including *Helicobacter pylori* (HopQ), *Neisseria meningitis* and *Neisseria gonorrhoeae* (colony opacity-associated, Opa proteins), *Haemophilus influenza* (Omp P1 protein), *Streptococcus agalactiae* (β-protein) and *Streptococcus pyogenes* (R28) (Baranov and Hammarström. 2004; Königer et al. 2016; Kuespert et al. 2011; Mix et al. 2021; Catton et al. 2023). While various studies have confirmed that *A. baumannii* can attach to human epithelial cells in the lungs and skin, the insights into the host-pathogen interaction involving adhesins like Bap that may facilitate *A. baumannii* colonization and internalization are not yet well established (Chen et al. 2022; Maure et al. 2023). Contradictory to these studies, an in vitro study showed that five *A. baumannii* and six *A. pittii* isolates of clinical origin failed to adhere and induce cytotoxicity to lung epithelial cells (Lázaro-Díez et al. 2016).

In this study, we attempt to identify differences among types of Bap to understand the evolutionary changes among *A. baumannii* that may favor biofilm formation and, subsequently, the pathogenesis. Further, using *in silico* approaches, we predicted the partial structure of the Bap protein, comprising multiple domains, and studied their interaction with human CEACAM-1 present on the epithelial cells and polymeric immunoglobulin receptor (PIgR) expressed on the mucosal surface of epithelial cells of pharynx and gut region. These interactions may induce a chain of signaling cascades that may benefit the pathogen by allowing it to survive during adhesion and evade immune response.

Methods

Retrieving genome sequences and classification based on bap type

Genome sequences of 7338 *A. baumannii* isolates available on the NCBI database until Feb 2023 were downloaded. tBlastn was performed to elucidate the distribution of different types of BAPs among the *A. baumannii* population. Query sequences for different types of Bap were obtained from a previous study (De Gregorio et al. 2015). An identity score of 90% or higher was used to select Bap sequences for analysis. The isolation source of isolates was also recorded from the NCBI database. Further, the Sequence Type (ST) of strains was determined according to the Pasteur scheme using the genome sequence as input on online

available tool Public databases for molecular typing and microbial genome diversity (https://pubmlst.org/organisms/acinetobacter-baumannii).

Physicochemical analysis of types of Bap

Physicochemical characterization of different types of Bap was performed using ExPASy ProtParam online tool (https://web.expasy.org/protparam/) (Gasteiger et al. 2005). Different types of Baps were compared on the basis of a number of amino acids, molecular mass, isoelectric point, aliphatic index, grand average of hydrophobicity (GRAVY), instability index, extinction coefficient, and Type-1, Type-2, and Type-3 Bap were compared based on these factors. The amino acid composition of Bap was also recorded.

Phylogenetic tree construction

The phylogenetic tree was constructed using the Bap amino acid sequence of 232 isolates, including strain AB5075 (with complete level genome sequence available at NCBI database) using the EMBL-EBI simple phylogeny online tool (https://www.ebi.ac.uk/Tools/phylogeny/simple_phylogeny). The data generated by the EMBL-EBI simple phylogeny tool was used to generate a diagram for a phylogenetic tree using iTol (https://itol.embl.de/).

Prediction of domain and motif function

Bap domains were predicted using amino acid sequences using the InterPro tool (https://www.ebi.ac.uk/interpro/), which predicts the family and superfamily of a particular domain. The predicted domains were further analyzed to identify the conserved sequences and evolutionary relationships. Motif Scan (https://myhits.sib.swiss/cgi-bin/motif_scan) was used to identify all the motifs occurring in Bap with the primary amino acid sequence as the input. Pfam database and Hidden Markov Model-based profiles were employed for scanning motifs in the Bap sequence.

In silico tertiary structure modelling using protein threading

The three-dimensional structure of types of Bap was predicted by protein threading using the Iterative Threading ASSEmbly Refinement (I-TASSER) tool, an online software that predicts structure based on multiple threading alignments, Local Meta- Threading Server (LOMETS). The amino acid sequence of a single copy of each multiple repeat sequence representing an immunoglobulin-like domain comprising the protein was used as input to generate the predicted structure (Wollacott et al. 2007). Five closest stereochemical structures were obtained, and the confidence of each model was quantitatively measured by confidence (C)-score. A higher C-score signifies higher confidence in the model. Subsequently, the quality of the structure was estimated by the C, template modelling (TM), and root mean deviation score (RMDS) scores.

Validation of predicted structures

The structures predicted by I-TASSER were further validated by using the online available SAVEs tool, which comprised of programs such as ERRAT (Colovos C and Yeates TO. 1993), VERIFY 3D (Bowie et al. 1991; Lüthy et al. 1992); and the stereochemical quality of protein was determined by analyzing the orientation of dihedral angles (torsion) angles phi (Φ) and psi (ψ) by generating Ramachandran Plot using PROCHECK analysis tool (Laskowski et al. 1998).

Prediction of protein-protein interaction of Bap and host carcinoembryonic antigen cell adhesion molecules (CEACAM-1) and polymeric immunoglobulin receptor (PIgR)

The interaction of Bap with CEACAM-1 and PIgR was performed using HDock online software (https://hdock.phys.hust.edu.cn/). The modelled structure of Bap generated by I-TASSER was used as a receptor, and the structure of CEACAM-1 (PDB ID: 4QXW) and PIgR (PDB ID: 1xed) available on RCSB Protein Data Bank was used. The top 10 structures predicting the interaction of host protein and Bap were displayed. The structure with the correct interaction stereochemistry was selected for further analyzing the interacting residues by LigPlot^{+} v.2.2.

Statistical analysis

GraphPad Prism version 5.1 was used for all the statistical analysis and plotting graphs. One-tailed t-test was used to analyze the differences in physicochemical properties among different Bap Types.

Result and discussion

Baps correlation with isolation source and sequence type (ST) in *A. baumannii* population

The biofilm-associated protein of *A. baumannii* includes a diverse range of Bacterial Immunoglobulin (BIg) domains that facilitate biofilm formation on abiotic and biotic surfaces. Bap contributes to *A. baumannii* pathogenesis by

adhering to host epithelial cells. Initially, we determined the distribution of Bap among 7,338 *A. baumannii* genome sequences available on NCBI database until Feb 2023. The presence and classification of Bap were determined using tBlastn with query sequence reported previously by De Gregorio et al. 2015 on the extensive characterization of the genetic organization of Bap (De Gregorio et al. 2015). tBlastn results revealed that 87.52% (6,422) of analyzed sequences harbor heterogeneous Bap. Based on the amino acid composition described previously, *A. baumannii* genomes featuring Type-1, Type-2, and Type-3 Bap were classified and encoded by 12.12%, 68.44%, and 6.91%, *A. baumannii* strains, respectively (Fig. 1a). Type-6 or SDF-Type was found in 0.054% of *A. baumannii* strains, while 12.51% lacked the Bap or biofilm-like proteins (BLP) genes (Fig. 1a). Type-2 Bap differed from Type-1 due to the presence of Ig-like repeat, Z, distinct from D repeat identified in Type-1, while Type-3 Bap diverged from Type-1 and Type-2 with only 30–40% similarity in the amino acid sequence of the carboxyl terminal, at the end of G domain. (De Gregorio et al. 2015).

Further, we analyzed the isolation source of *A. baumannii* to determine if the presence of a particular Bap type is associated with specific clinical manifestations. The majority of *A. baumannii* strains carrying Type-1 Bap were retrieved from respiratory specimen (23.172%) and bloodstream (15.80%). Similarly, *A. baumannii* isolates encoding for Type-2 Bap were also predominantly obtained from respiratory specimens (34.42%) and bloodstream (13.97%). A significant proportion of *A. baumannii* carrying Type-3 Bap were primarily isolated from respiratory specimens (25.83%) and environment (12.82%). However, the isolation source of *A. baumannii* harboring Type-1, Type-2, and Type-3 of 22.94%, 33.07%, and 9.8% isolates, respectively, was not defined. These findings suggest that *A. baumannii* is more likely to infect upper respiratory tissues and organs, regardless of the Bap type, which is consistent with previous studies (Alsan and Klompas 2010; Howard et al. 2012; Zilberberg et al. 2016). The second significant infection site in the case of strains with Type-1 and Type-2 Bap was found to be blood or catheter-associated infections (Alsan and Klompas 2010). In contrast, many isolates (12.82%) harboring Type-3 Bap were also isolated from the environment (Fig. 1b).

Multilocus sequence typing (MLST) was analyzed at *A. baumannii* MLST website using the Pasteur scheme. In total, 889 isolates harboring Type-1 Bap belong to 113 different sequence types, and we found that ST1 and ST295 exclusively harbored Type-1 Bap with 20.80% and 11.58% isolates, respectively. Similarly, isolates presenting Type-2 Bap belong to 316 different STs, but 55.47% of the population belongs to ST2. In the case of isolates harboring Type-3 Bap, ST25 was more predominant with 33.92% of isolates (Fig. 1c). *A. baumannii* strains belonging to ST92, 296, 307, 318, 328, and 499 were mutual among all three Bap types. However, it was observed that isolates belonging to a particular ST were associated with a particular type of Bap, suggesting a correlation between the genetic background of bacterial strain, as characterized by its ST and the Bap variant it carries. Instances where ST has less than 10 isolates and conceals a single type of Bap are not shown in Fig. 1c. A previous study showed that strains belonging to ST2, ST25, and ST78 have a higher ability to form a biofilm (Giannouli et al. 2013). A separate study observed that sporadic strains had a significantly higher ability to form biofilms than epidemic isolates associated with ST2 (Hu et al. 2016).

Bap plays a crucial role in the evolution of virulent *A. baumannii*

Neighbor-Joining (NJ) tree was constructed using Bap amino acid sequences of isolates belonging to Type-1 (n = 68), Type-2 (n = 92), Type-3 (n = 70), and SDF-Type (n = 2). Type-1 Bap was the most ancient, followed by Type-2 and Type-3. SDF shared the common ancestors with Type-1 (Fig. 2a). Domain analysis of Bap protein among *A. baumannii* using InterPro server revealed five major domains, VCBS (*Vibrio*, *Colwellia*, *Bradyrhizobium*, and *Shewanella*), BapA, Bacterial immunoglobulin-like domains 6, 12, and 13 (BIg6, BIg12, and BIg13). BIg12 (Pfam ID-19078) and BIg13 (Pfam ID-19077) domains are also present in multiple tandem copies and are associated with bacterial surface proteins. SDF Type Bap exclusively comprised of only the BIg6 domain (Pfam ID-17936), reported in several extracellular proteins produced by bacteria and is found in multiple consecutive repeats. These bacterial domains have been reported in various extracellular bacterial proteins and are crucial for adhesion (Chatterjee et al. 2021). Further, we analyzed the conserved amino acid residues among different domains using the NCBI COBALT tool (Fig. 2b, c). The amino acid sequence "DADGTVGTGTVDADGTFS" and QANGE-TLSVTA—TDAAGNVSPA" among BIg6, BIg12, BIg13, BapA, and VCBS domain; amino acids SDDGTTLTGTGEAG, ATVTVT, DADGTVGTGTVDADGTFS, FTPTAAVA-GAT-TLTVTA, and TDLAGNAGTG among BIg6, BIg12, and BIg13 were found to be conserved (Fig. 2c). Upon analyzing the neighborhood trees of these domains, it was found that BIg6 and BIg12 exhibited closer relationship, than BIg13 and VCBS (Fig. 2b).

The presence of sialate O-acetylesterase domain was analysed among 232 Bap sequences. Several sequences of Type-1 ($n = 39/68$; 57.35% of Type-1), Type-2 ($n = 34/92$; 36.95% of Type-2) and Type-3 ($n = 4/70$; 5.71% of

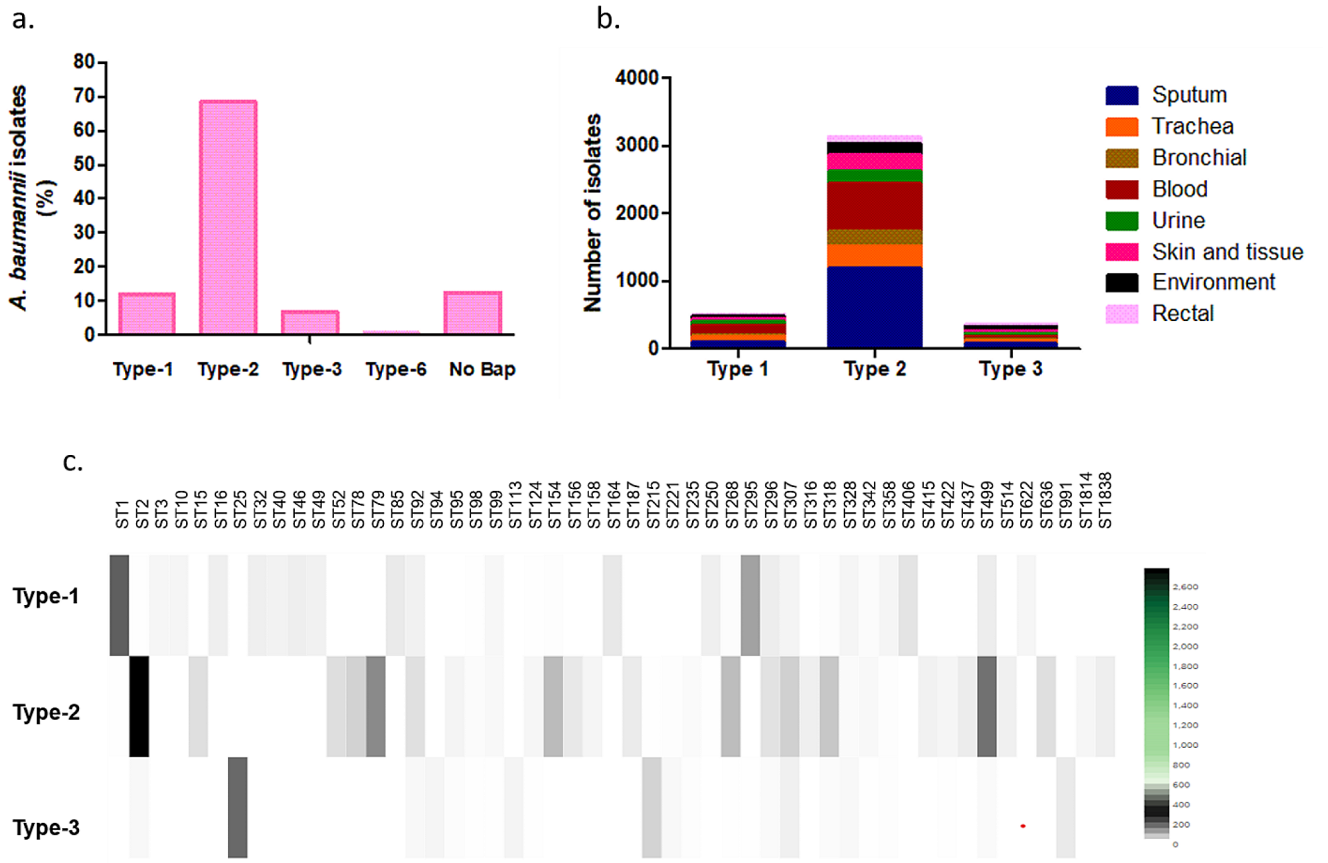

Fig. 1 **(a)** Distribution of Type-1, Type-2, and Type-3 BAP among various sequence types of *A. baumannii*. **(b)** Isolation source of *A. baumannii* harboring Type-1, Type-2, and Type-3 Bap. **(c)** Number of *A. baumannii* isolates with Type-1, Type-2, and Type-3 Bap belonging to different ST. Majority of isolates with Type-1, Type-2 and Type-3 Bap belong to ST1, ST2 and ST25, respectively

Type-3) Bap were found, including the most recent strain ACIN00156 containing sialate O-acetylesterase domain (Pfam ID- IPR039329). Bacteria possessing O-acetyl sialate esterase(s) employ acetylated sialic acids as a source for growth, potentially securing a metabolic advantage over rivals that do not exhibit this enzymatic activity (Rangel et al. 2016). The sialidase activity is also responsible for the degradation of the mucosal barrier in the respiratory tract to promote pneumonia as reported during *S. pneumoniae* infection (Kahya et al. 2017). It can be hypothesized that the evolution of *A. baumannii* Bap could also have an immunomodulatory role during human infection.

Variations in the physicochemical properties of baps

The physicochemical analysis of different types of Bap encoded by 201 representative strains (57 Type-1, 69 Type-2, 75 Type-3) using Expasy ProtParam revealed the heterogeneity of this protein. Significant differences in molecular weight, isoelectric point, and instability index were observed among Type-1, Type-2, and Type-3 Bap (Fig. 3). Bap among *A. baumannii* was found in molecular weights ranging from 73.930 kDa to 872.555 kDa of strain XH960 and 9120, respectively. The isoelectric point (pI) of the protein ranged from 2.74 to 4, indicating the overall negative charge and acidic nature of the protein. The Type-1 Bap proteins were highly stable with an instability index ranging from 3.58 to 6.73, Type-2 ranging from 5.1 to 10.56, Type-3 ranged from 12.04 to 32.4, and the Type 6 Bap was unstable with an instability index of 59.65 to 67.62 for strains SDF, AB046, AB048 and AB053 (not shown). Type-1 Baps encoded by *A. baumannii* were found to have the highest average molecular weight (670935.88 ± 163028.54 Da), lowest isoelectric point (3.15 ± 0.06), and higher stability (Instability index = 4.83 ± 0.90). In comparison, Type-2 and Type-3 Bap had significantly lower average molecular weight (480149.94 ± 190419.45 Da and 249574.84 ± 134585.79 Da, respectively), higher isoelectric point (3.42 ± 0.18 and 3.57 ± 0.16) and were less stable (with instability index of 8.12 ± 1.64 and 15.46 ± 4.80), respectively (Fig. 3a, b, c). Grand average of hydropathicity (GRAVY) of Type-1 BAP protein was 0.071 to 0.168. Type-2 0.079 to 0.193, Type-3 -0.188 to 0.271 (Fig. 3d). The wide-ranging differences in GRAVY of Bap among *A. baumannii* show that the protein

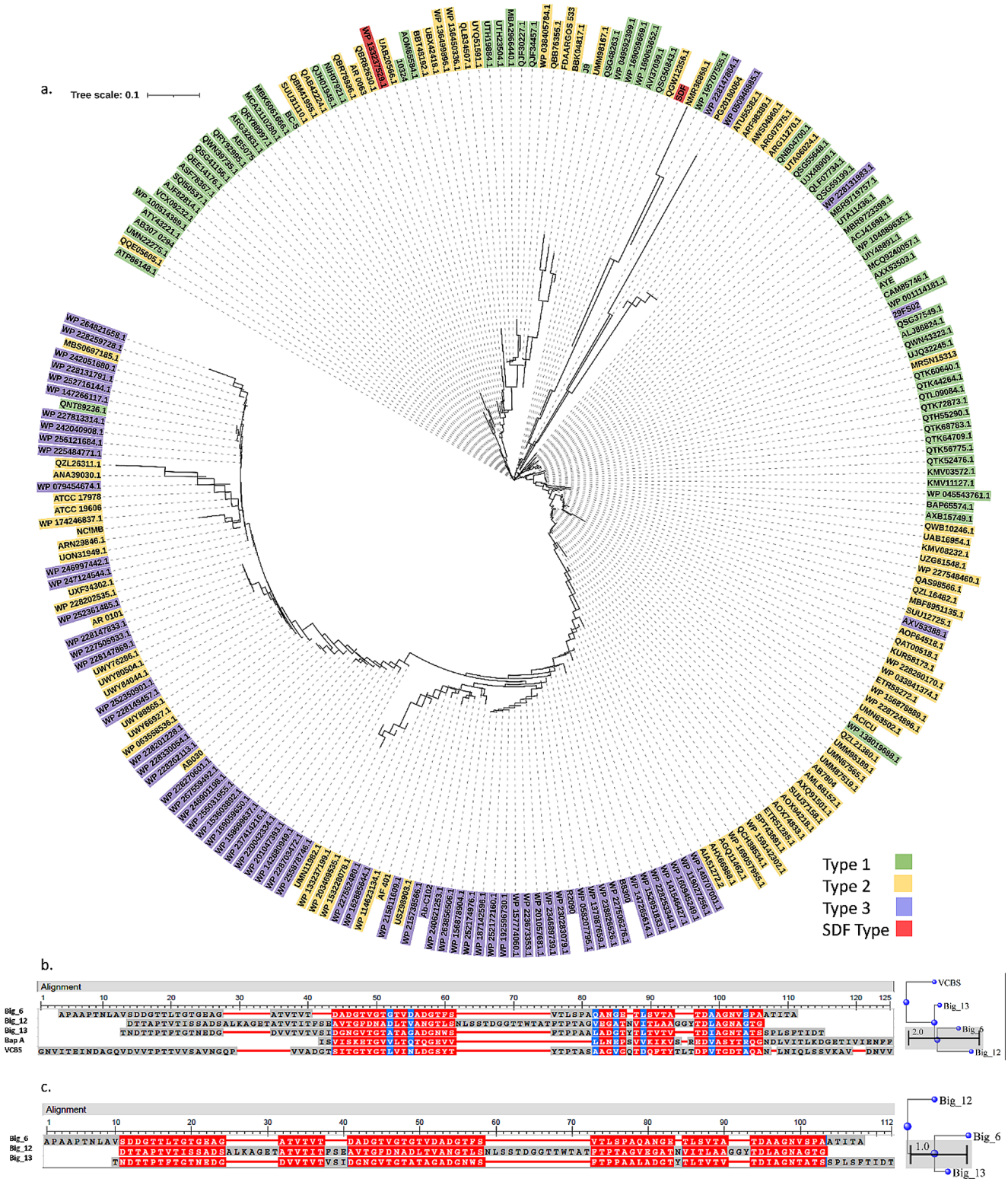

Fig. 2 **a.**Phylogenetic tree analysis of Bap types. The protein sequence code in green belongs to Bap Type-1, Type-2 is depicted with yellow, and Type-3 and SDF type are shown in violet and red, respectively. **b** and **c**. Highly conserved and less conserved amino acid positions based on relative entropy threshold among identified Bap domains are highlighted in red and blue, respectively. The neighbor-joining tree of identified Bap domains showed that VCBS and BIg13 are more closely related. **c.** and BIg6, and BIg13, were more closely and distantly related to BIg12

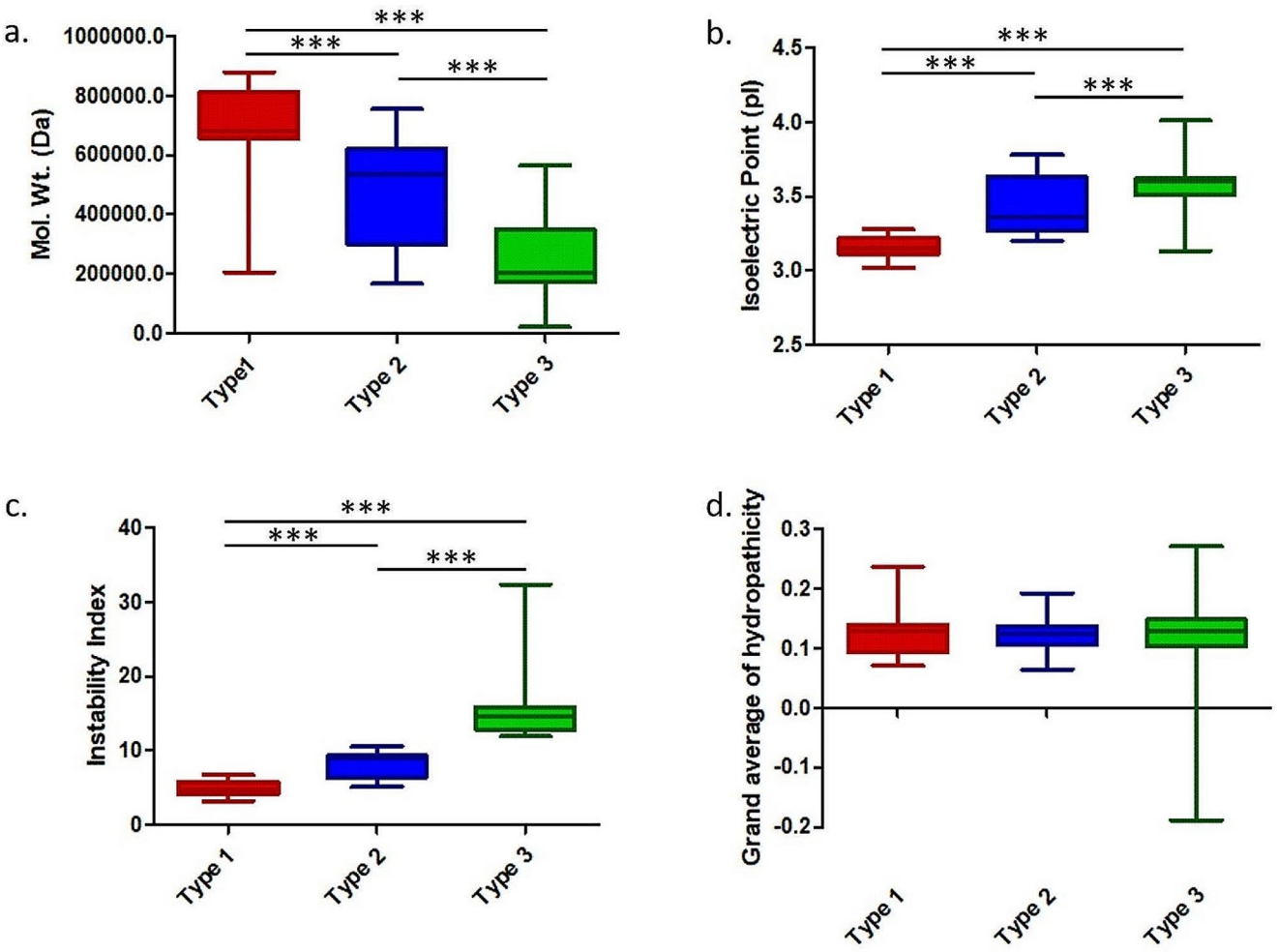

Fig. 3 Differences in physicochemical properties of Type-1, Type-2, and Type-3 Bap on the basis of their (**a**) Molecular weight, (**b**) Isoelectric point, (**c**) Instability index and (**d**) Grand average of hydropathicity (***, p value < 0.001)

can be either hydrophilic or hydrophobic isolates. Although most Bap variants, including Type-1 and Type-2, were hydrophobic, some strains encoded for hydrophilic Type-3 and Type-6 Bap.

Analysis of the amino acid composition of Baps showed that threonine, a hydrophilic amino acid containing the hydroxyl group in its side chain, was the most abundant amino acid in Type-1, -2 and −3 Bap accounting for 12.4–18.5% of amino acids within the analyzed protein sequences (Fig. 4a). This observation aligns with previous findings, although the specific significance of the abundance of threonine remains undefined (Yousef et al., 2007). Later, it was postulated that phosphorylation on the hydroxyl group of threonine may play a role in pathogenesis during adherence on host cells, however, further investigation is required (Ribet and Cossart 2010). The percentage of threonine in Bap Type-3 was significantly less than that of Type-1 (p-value = 0.0333) and Type-2 (p-value = 0.0261) (Fig. 4b). Serine, (containing hydroxyl group) was found to have significantly higher levels in Type-3 (p-value = 0.0040) and Type-2 (p-value = 0.0172) as compared to Type-1 Bap (Fig. 4c). Leucine, a non-polar, aliphatic amino acid, was also significantly abundant in Type-3 Bap as compared to Type-1 (p-value = 0.0082) and Type-2 (p-value = 0.0133) (4d). Since we found increased levels of leucine in Type-2 and Type-3 Bap, we screened Bap sequences for leucine-rich repeats (LRR) and found that Type-2 and Type-3 Bap contained 4–5 LRR motifs at the carboxyl-terminal region of Bap. These LRR might play role in mediating protein-protein interactions. Further studying the role of these amino acids among different Baps would provide valuable insights into their role during host-pathogen interaction. Besides that, hydrophobic amino acids glycine, alanine, and valine were found to be conserved among these three Baps. Negatively charged aspartate and glutamate constituted 9-11.5% and 1.4–3.2% of the protein, respectively. Sulphur containing amino acid cysteine was completely absent, but methionine was found in traces constituting 0.1–0.5% of the protein.

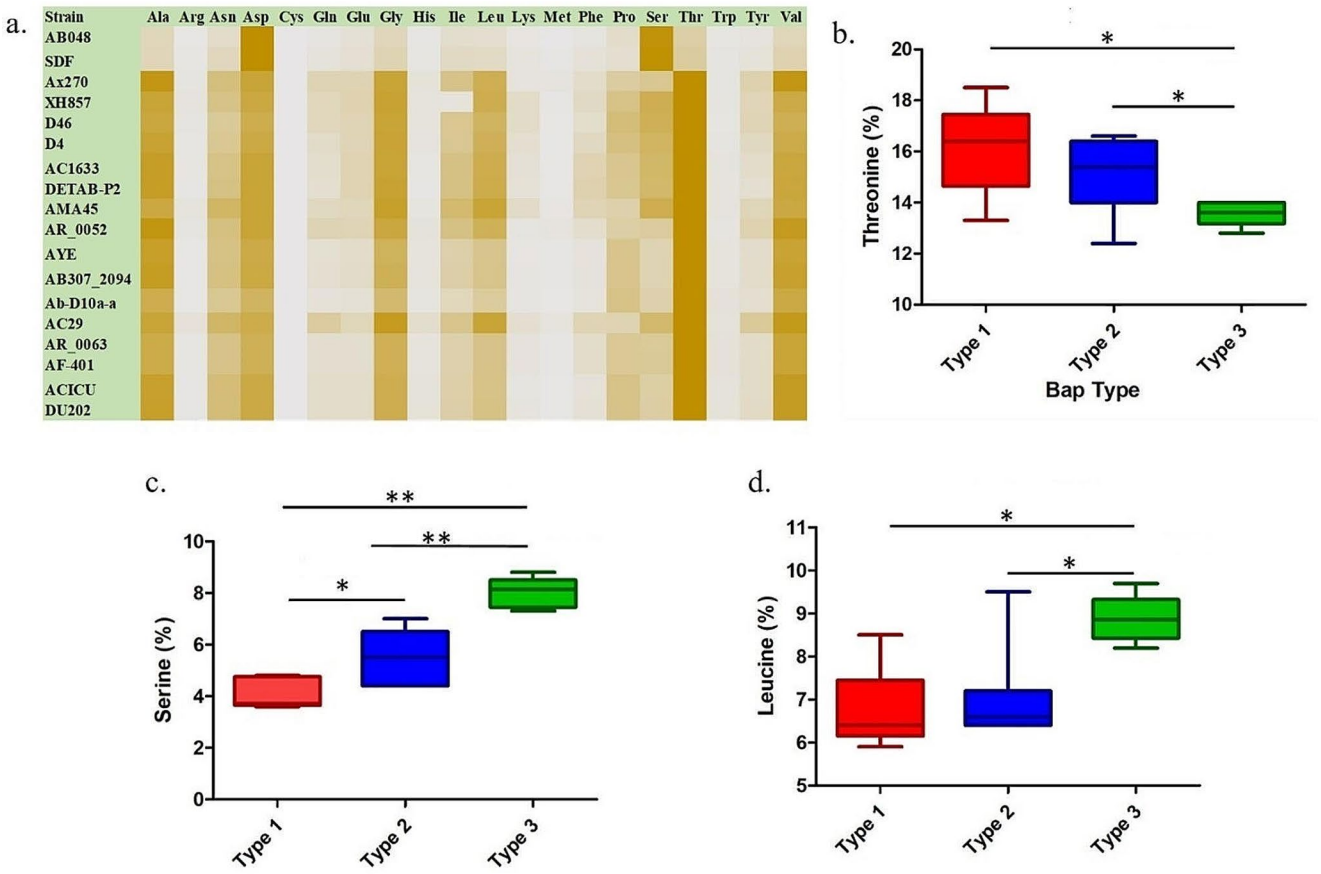

Fig. 4 **(a)** Variations in amino acid composition among Bap/s. **(b)** Significant reduction of threonine, with the increase in **(c)** serine and **(d)** leucine percentage among Baps with its evolution. (**, p value < 0.01; *, p value < 0.05)

In silico structure modelling of Baps

The experimental three-dimensional structure of Bap of *A. baumannii* is yet to be reported. For predicting the 3-D structure of each type of Bap, the repeats from the same type of Bap constituting different types of domains were merged into a single sequence, and the structure was predicted using I-TASSER. For each sequence submitted, I-TASSER generated the five most favorable structures based on protein threading. Structures with the highest Ramachandran favored score were selected (Fig. 5). The estimated TM score, estimated RMSD, and Ramachandran score of each selected structure are mentioned in Table 1. The predicted structure revealed that the multi-domain structure comprised antiparallel β-sheets constituting the β-sandwich domain. The multiple subunits were linked with the alpha-helical structures constituting the multi-domain structure of the protein.

Evolution of Bap facilitates improved interaction with CEACAM-1 and PIgR

Previous studies have shown that Bap facilitates *A. baumannii* adhesion to human epithelial cells, and another study found that *A. baumannii* strain 5075 that contains Type-1 Bap (sequence ID: AKA30645.1) interacts with the CEACAMs receptors (Brossard and Campagnari 2012; Ambrosi et al. 2020). BAP sequence of the *A. baumannii* isolate AYE (GenBank ID: CAM85746.1) was used as the representative sequence for investigating the interaction of Type-1 BAP and CEACAM. Bap of this isolate exhibits 95% sequence similarity with that of strain AB5075. CEACAMs have been found as target molecules by various pathogens, such as capsule-producing *N. meningitidis*, *H. influenzae*, and *Moraxella catarrhalis*, that infect the nasopharynx (Villullas et al. 2007). Interaction of opportunistic pathogens with CEACAMs has led to tissue invasion and migration across the epithelial layer (Hill et al. 2005; Sheikh and Fleckenstein 2023). The BIg13 domain and BIg6 domain of Type-1, -2, -3, and SDF-Type Bap, respectively, were found to target the N-terminal dimer of CEACAM-1 receptor by hydrophobic interactions and ionic interactions. The BIg 13 domain of AYE was 100% similar to that of strain AB5057, that was previously shown to interact with CEACAMs. This finding corroborated with the earlier observations where the BIg13 domain of the R28 receptor expressed on the surface of *Streptococcus pyogenes*, which causes puerperal sepsis and other Gram-positive bacteria expressing BIg13 interacts

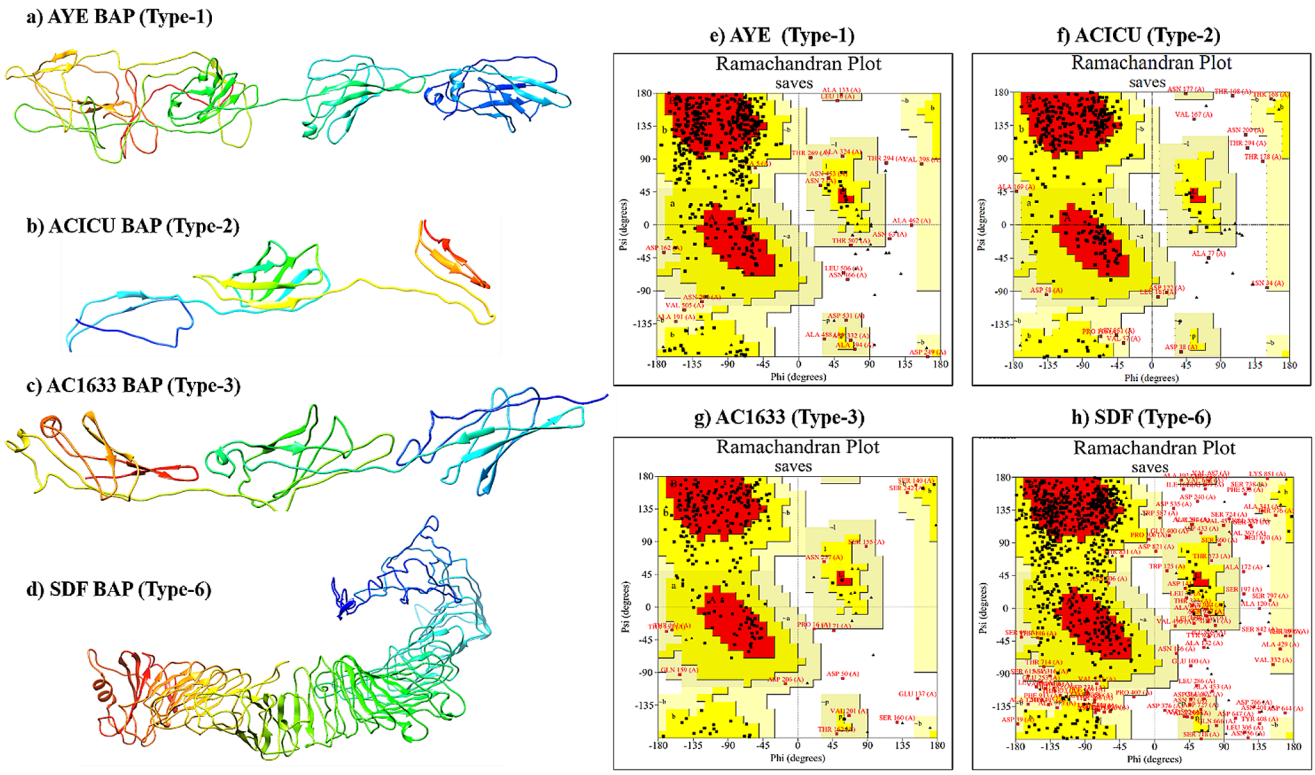

Fig. 5 Predicted 3-Dimentional structures comprising single unit of multiple repeats: (**a**) AYE (Type-1), (**b**) ACICU (Type-2), (**c**) AC1633 (Type-3), (**d**) SDF (Type-6) and their Ramachandran plots (**e, f, g** and **h**, respectively)

Table 1 Validation scores of predicted 3D structures of types of Bap

Strain	AYE (Type-1)	ACICU (Type-2)	AC1633 (Type-3)	SDF (Type-6)
Estimated TM score	0.55 ± 0.15	0.68 ± 0.12	0.62 ± 0.14	0.52 ± 0.15
Estimated RMSD	10.6 ± 4.6Å	5.8 ± 3.6Å	7.9 ± 4.4Å	12.8 ± 4.2Å
Residues in most favoured region (%)	61.9	71.8	62.5	50.9
Residues in additionally favoured region(%)	33.2	22.8	31.9	37.1
Residues in generously allowed region (%)	3.7	3.4	4.0	8.2
Residues in disallowed region(%)	1.3	2	1.6	3.8
Verify 3D (%)	62.99	72.80	57.79	55.16
Errat score	66.74	66.76	65	52.3
Alpha helix (%)	0	2.20	6.49	8.10
Random coil (%)	69.22	54.12	45.78	42.41
Beta strand (%)	30.78	37.36	36.04	39.07
Beta turn (%)	0	6.32	11.69	10.43

with dimeric CEACAM-1 receptor (Catton et al. 2023; van Sorge et al. 2021). Three residues of both the N-terminal chains of dimeric CEACAM-1 (Asn^{23}, Glu^{37}, $Asn^{81}$of chain B and Asn^{81}, Arg^{43}, and Asp^{40} of Chain C) interacted with Gly^{221}, Val^{169}, Asp^{162}, Asn^{200}, Asp^{164} and Thr^{167} of BIg13 domain of AYE Bap along with several other hydrophobic interactions (Supplementary Material, Fig. S1). In the case of docking between ACICU Bap and CEACAM, interactions between Asp^{125} and Arg^{38} of chain B and Asp^{125}, Ser^{123}, Asp^{99}, Thr^{119}, and Leu^{50} interacted with Arg^{38}, Arg^{43}, Thr^{83}, Val^{106}, and Gln^{103} of chain B of CEACAM-1 (Supplementary Material, Fig. S2). Interaction between Type-3 Bap of AC1633 and CEACAMs involved the highest number of residues among all the Bap types. Ser^{93}, Ala^{2}, Asn^{88}, and Ser^{90} interacted with Arg^{38}, Gln^{103}, and Glu^{37} of Bap and CEACAM-1, respectively (Fig. 6a). Since *A. baumannii* majorly infects the respiratory tract, specifically the nasopharynx region, it was of interest to understand the interaction of Bap with PIgR that mediates the secretion of antibodies on the mucosal lining of the nasopharynx region. Using the HDock tool online, *in silico* docking of Bap with PIgR showed that Bap interacts with different binding

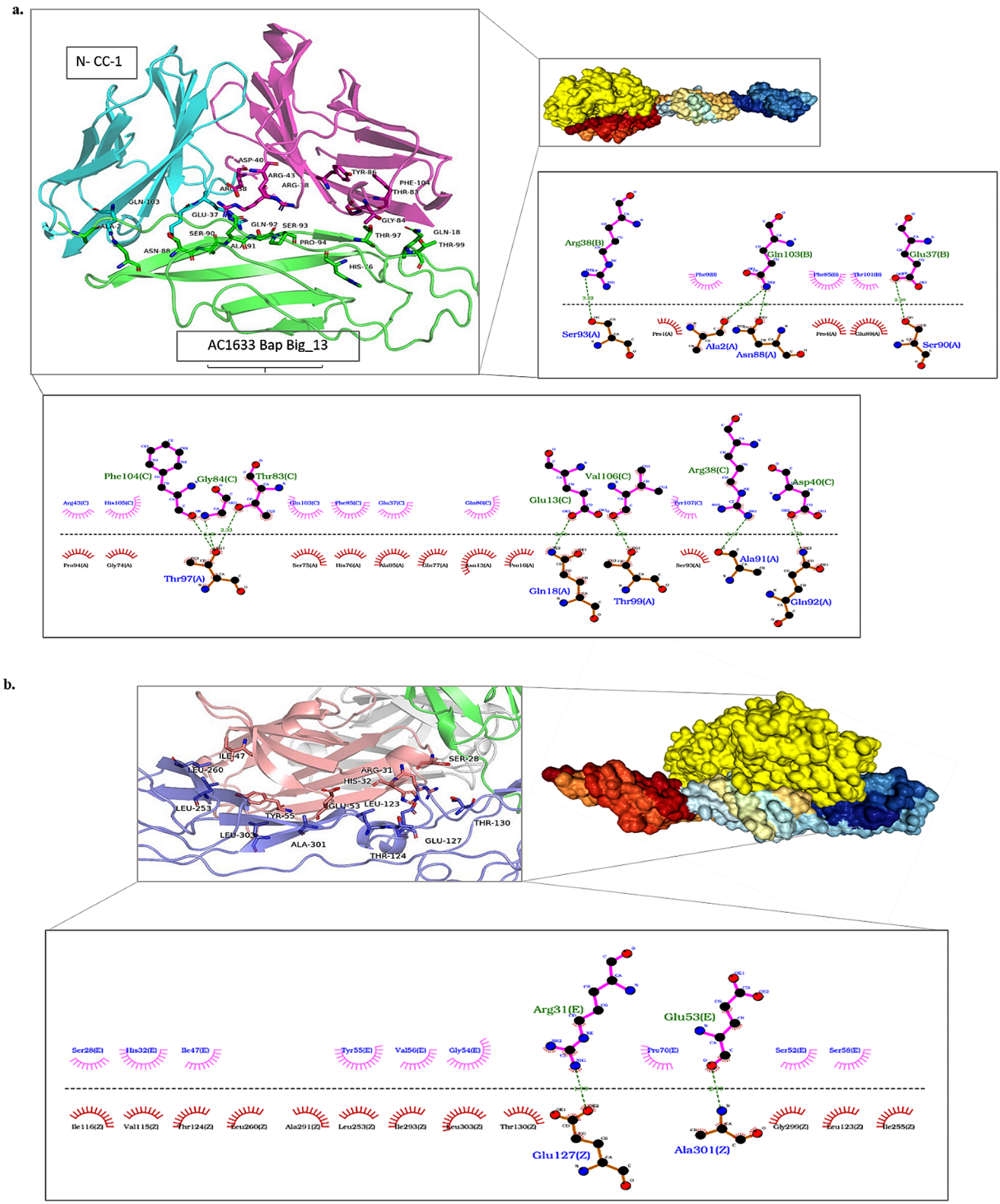

Fig. 6 **(a)**The figure illustrates the interaction between predicted 3-D structure of Type-3 Bap (chain A) of *A. baumannii* isolate AC1633 and N-terminal of human CEACAM-1 (chain B and C) via its BIg13 domain **(b)** Predicted 3-D structure of Type-3 Bap (Chain Z) of *A. baumannii* isolate AC1633 shows interaction with E domain of PIgR (Chain E) using hybrid docking strategy. The interface residues predominantly showed hydrophobic and ionic interactions.

Table 2 Summary of docking models

Host Receptor	CEACAM-1				PIgR			
Bap type	AYE (Type-1)	ACICU (Type-2)	AC1633 (Type-3)	SDF (Type-6)	AYE (Type-1)	ACICU (Type- 2)	AC1633 (Type-3)	SDF (Type-6)
Docking Score	-251.65	-210.85	-224.84	-265.82	-254.16	-243.51	-299.85	-318.56
Confidence Score	0.8843	0.7715	0.8171	0.9102	0.8893	0.8665	0.9524	0.9668
Ligand RMSD	198.97	123.37	179.64	139.70	215.55	120.93	162.31	146.69

energies. It was observed that all types of Bap interact with the CEACAM-1 receptor and PIgR but with varying binding energies and interacting residues. Table 2 summarizes the binding energies of interaction studies and docking parameters. A previous study also showed that *Streptococcus pneumoniae* interacts with PIgR, specifically with its choline-binding protein A (Brock et al. 2002). Another study showed that a pneumococcal surface protein, *pspC*, interacts with PIgR and facilitates the invasion of *S. pneumoniae* into host cells (Agarwal et al. 2010). The amino acid residues Thr, Asp, Ala, and valine of Bap involved in interaction with CEACAM-1 and PIgR reflect the reason for their abundance in the protein (Fig. 6b). Analyzing the differences in the interaction of Baps with CEACAM-1 and PIgR, it can be hypothesized that *A. baumannii* Bap is evolving to facilitate the enhanced virulence of this pathogen. Previous studies have shown that *A. baumannii* Bap facilitates adhesion to human bronchial epithelial and neonatal keratinocyte cells but inhibits intracellular invasion of *A. baumannii* in these cells (Brossard and Campagnari 2012). To advance our understanding of *A. baumannii*'s invasion of host cells, further research on the potential of different Bap types is crucial. Identifying the specific domains responsible for this mechanism and studying the role of different Bap types in eliciting varied immune responses would pave the way for developing targeted therapeutics. Such studies would significantly contribute to the development of effective treatment options for *A. baumannii* infections.

Conclusion

A. baumannii, once considered non-pathogenic, has rapidly transformed into a significant contributor to healthcare-associated and community-acquired infections. The biofilm-forming ability has played a significant role in transforming *A. baumannii* into a pathogen and in the development of multidrug resistance. However, our understanding of mechanisms underlying *A. baumannii* infection and interactions with the host contributing to its pathogenicity is inadequate. In this study, using *in silico* approaches, we illustrated the structural aspects of biofilm-associated protein that play a crucial role in establishing and forming mature biofilms during infection. This study reports the differences in Bap types by predicting their partial structure, amino acid composition, physicochemical properties, and domain analysis. Furthermore, we speculated the differences in their ability to interact with the host CEACAM-1 and PIgR receptors and found that the recently evolved Bap Type-3 showed more efficient interaction, thus advancing our knowledge about the pathogenesis of this rapidly evolving pathogen. *A. baumannii* strain AB5075 has been shown to interact with the CEACAMs, previously (Ambrosi et al. 2020). Our analysis revealed that strain AB5075 carried Type-1 Bap with sequence ID AKA30645.1, depicted in the phylogenetic tree. However, future studies should focus on the role of Bap mediating this interaction and internalization of *A. baumannii*. Investigating the impact of elevated levels of serine and leucine, precisely leucine-rich repeats identified in the carboxyl region of some Type-2 and Type-3 Bap will offer insights into their regulatory mechanisms or their function in adhesion. Since the BIg13 domain played a major role in facilitating Bap-CEACAM-1, constructing BIg13 mutants and its impact on biofilm formation ability on biotic and abiotic surfaces would be important. It would be helpful to study the interaction between Bap and PIgR to understand the strategies used by *A. baumannii* to evade the immune system, which can contribute to its ability to cause disease. By examining the role of Bap domains in invading host cells and evading the immune system, we can gain insights into developing targeted therapies. Further research is needed to understand the signaling cascade resulting from this interaction, which could give the pathogen an advantage by facilitating its survival during initial adhesion and allowing it to evade the host's immune responses.

Discovering the evolutionary and pathogenic role of *A. baumannii* Bap is a critical step in developing targeted therapies against this dangerous pathogen. Using *in silico* approaches, this study successfully characterizes Bap and unravels its crucial role through detailed structure modelling. The findings of this study have significant implications for the development of more effective treatments against *A. baumannii* infections.

Supplementary Information The online version contains supplementary material available at https://doi.org/10.1007/s00203-024-03992-8.

Acknowledgements This work was supported by ICMR-National Institute of Pathology, New Delhi, India. KU acknowledges the University Grant Commission (UGC), New Delhi, India, for providing fellowship.

Author contributions KU, RK, QMR, and RS conceived and designed the study. KU and RK performed the experiments. KU, RK, and RS analyzed the data. KU RK and RS drafted the manuscript. All authors reviewed and approved the manuscript.

Funding ICMR-National Institute of Pathology.

Data availability No datasets were generated or analysed during the current study.

Declarations

Competing interests The authors declare no competing interests.

References

Agarwal V, Asmat TM, Dierdorf NI, Hauck CR, Hammerschmidt S (2010) Polymeric immunoglobulin receptor-mediated invasion of Streptococcus pneumoniae into host cells requires a coordinate signaling of SRC family of protein-tyrosine kinases, ERK, and c-Jun N-terminal kinase. J Biol Chem 285(46):35615–35623. https://doi.org/10.1074/jbc.M110.172999

Alsan M, Klompas M (2010) *Acinetobacter baumannii*: an emerging and important pathogen. J Clin Outcomes Management: JCOM 17(8):363

Ambrosi C, Scribano D, Sarshar M, Zagaglia C, Singer BB, Palamara AT (2020) *Acinetobacter baumannii* targets human carcinoembryonic antigen-related cell adhesion molecules (CEACAMs) for invasion of pneumocytes. Msystems 5(6):10–1128. https://doi.org/10.1128/msystems.00604-20

Bamberger AM, Sudahl S, Löning T, Wagener C, Bamberger CM, Drakakis P, Coutifaris C, Makrigiannakis A (2000) The adhesion molecule CEACAM1 (CD66a, C-CAM, BGP) is specifically expressed by the extravillous intermediate trophoblast. Am J Pathol 156(4):1165–1170. https://doi.org/10.1016/S0002-9440(10)64985-1

Baranov V, Hammarström S (2004) Carcinoembryonic antigen (CEA) and CEA-related cell adhesion molecule 1 (CEACAM1), apically expressed on human colonic M cells, are potential receptors for microbial adhesion. Histochem Cell Biol 121:83–89. https://doi.org/10.1007/s00418-003-0613-5

Bowie JU, Lüthy R, Eisenberg D (1991) A method to identify protein sequences that fold into a known three-dimensional structure. Science 253(5016):164–170. https://doi.org/10.1126/science.1853201

Brock SC, McGraw PA, Wright PF, Crowe JE Jr (2002) The human polymeric immunoglobulin receptor facilitates invasion of epithelial cells by Streptococcus pneumoniae in a strain-specific and cell type-specific manner. Infect Immun 70(9):5091–5095. https://doi.org/10.1128/iai.70.9.5091-5095.2002

Brossard KA, Campagnari AA (2012) The *Acinetobacter baumannii* biofilm-associated protein plays a role in adherence to human epithelial cells. Infect Immun 80(1):228–233. https://doi.org/10.1128/iai.05913-11

Catton EA, Bonsor DA, Herrera C, Stålhammar-Carlemalm M, Lyndin M, Turner CE, McCarthy AJ (2023) Human CEACAM1 is targeted by a Streptococcus pyogenes adhesin implicated in puerperal sepsis pathogenesis. Nat Commun 14(1):2275. https://doi.org/10.1038/s41467-023-37732-1

Chapartegui-González I, Lázaro-Díez M, Bravo Z, Navas J, Icardo JM, Ramos-Vivas J (2018) Acinetobacter baumannii maintains its virulence after long-time starvation. PLoS ONE, 13(8), e0201961

Chatterjee S, Basak AJ, Nair AV, Duraivelan K, Samanta D (2021) Immunoglobulin-fold containing bacterial adhesins: molecular and structural perspectives in host tissue colonization and infection. FEMS Microbiol Lett 368(2):fnaa220. https://doi.org/10.1093/femsle/fnaa220

Chen CL, Dudek A, Liang YH, Janapatla RP, Lee HY, Hsu L, Kuo HY, Chiu CH (2022) d-mannose-sensitive pilus of *Acinetobacter baumannii* is linked to biofilm formation and adherence onto respiratory tract epithelial cells. J Microbiol Immunol Infect 55(1):69–79. https://doi.org/10.1016/j.jmii.2021.01.008

Colovos C, Yeates TO (1993) Verification of protein structures: patterns of nonbonded atomic interactions. Protein Sci 2(9):1511–1519. https://doi.org/10.1002/pro.5560020916

De Breij A, Eveillard M, Dijkshoorn L, Van Den Broek PJ, Nibbering PH, Joly-Guillou ML (2012) Differences in *Acinetobacter baumannii* strains and host innate immune response determine morbidity and mortality in experimental pneumonia. PLoS ONE 7(2):e30673. https://doi.org/10.1371/journal.pone.0030673

De Gregorio E, Roscetto E, Iula VD, Martinucci M, Zarrilli R, Di Nocera PP, Catania MR (2015) Development of a real-time PCR assay for the rapid detection of *Acinetobacter baumannii* from whole blood samples. New Microbiol 38(2):251–257

Eze EC, Chenia HY, El Zowalaty ME (2018) *Acinetobacter baumannii* biofilms: effects of physicochemical factors, virulence, antibiotic resistance determinants, gene regulation, and future antimicrobial treatments. Infection and drug resistance, pp 2277–2299

Gasteiger E, Hoogland C, Gattiker A, Duvaud SE, Wilkins MR, Appel RD, Bairoch A (2005) *Protein identification and analysis tools on the ExPASy server* (pp. 571–607). Humana press. https://doi.org/10.1385/1-59259-890-0:571

Gedefie A, Demsis W, Ashagrie M, Kassa Y, Tesfaye M, Tilahun M, Bisetegn H, Sahle Z (2021) *Acinetobacter baumannii* biofilm formation and its role in disease pathogenesis: a review. Infect Drug Resist 3711–3719. https://doi.org/10.2147/IDR.S332051

Giannouli M, Antunes LC, Marchetti V, Triassi M, Visca P, Zarrilli R (2013) Virulence-related traits of epidemic *Acinetobacter baumannii* strains belonging to the international clonal lineages I-III and to the emerging genotypes ST25 and ST78. BMC Infect Dis 13:1–11. https://doi.org/10.1186/1471-2334-13-282

Goh HS, Beatson SA, Totsika M, Moriel DG, Phan MD, Szubert J, Runnegar N, Sidjabat HE, Paterson DL, Nimmo GR, Lipman J (2013) Molecular analysis of the *Acinetobacter baumannii* biofilm-associated protein. Appl Environ Microbiol 79(21):6535–6543. https://doi.org/10.1128/AEM.01402-13

Greene C, Vadlamudi G, Newton D, Foxman B, Xi C (2016a) The influence of biofilm formation and multidrug resistance on environmental survival of clinical and environmental isolates of *Acinetobacter baumannii*. Am J Infect Control 44(5):e65–e71. https://doi.org/10.1016/j.ajic.2015.12.012

Greene C, Wu J, Rickard AH, Xi C (2016b) Evaluation of the ability of *Acinetobacter baumannii* to form biofilms on six different biomedical relevant surfaces. Lett Appl Microbiol 63(4):233–239. https://doi.org/10.1111/lam.12627

Hammarström S (1999) The carcinoembryonic antigen (CEA) family: structures, suggested functions and expression in normal and malignant tissues. In Seminars in cancer biology (Vol. 9, No. 2, pp. 67–81). Academic Press. https://doi.org/10.1006/scbi.1998.0119

Hill DJ, Edwards AM, Rowe HA, Virji M (2005) Carcinoembryonic antigen-related cell adhesion molecule (CEACAM)-binding recombinant polypeptide confers protection against infection by

respiratory and urogenital pathogens. Mol Microbiol 55(5):1515–1527. https://doi.org/10.1111/j.1365-2958.2005.04487.x
Howard A, O'Donoghue M, Feeney A, Sleator RD (2012) Acinetobacter baumannii: an emerging opportunistic pathogen. Virulence 3(3):243–250. https://doi.org/10.4161/viru.19700
Hu Y, He L, Tao X, Meng F, Zhang J (2016) Biofilm may not be necessary for the Epidemic Spread of *Acinetobacter baumannii*. Sci Rep 6(1):32066. https://doi.org/10.1038/srep32066
Jung SY, Lee SH, Lee SY, Yang S, Noh H, Chung EK, Lee JI (2017) Antimicrobials for the treatment of drug-resistant *Acinetobacter baumannii* pneumonia in critically ill patients: a systemic review and bayesian network meta-analysis. Crit Care 21(1):1–15. https://doi.org/10.1186/s13054-017-1916-6
Kahya HF, Andrew PW, Yesilkaya H (2017) Deacetylation of sialic acid by esterasespotentiates pneumococcal neuraminidase activity for mucin utilization, colonization andvirulence. PLoS Pathog 13, e1006263
Kale SD, Dikshit N, Kumar P, Balamuralidhar V, Khameneh HJ, Bin Abdul Malik N, Koh TH, Tan GGY, Tan TT, Mortellaro A, Sukumaran B (2017) Nod2 is required for the early innate immune clearance of *Acinetobacter baumannii* from the lungs. Sci Rep 7(1):17429. https://doi.org/10.1038/s41598-017-17653-y
Königer V, Holsten L, Harrison U, Busch B, Loell E, Zhao Q, Bonsor DA, Roth A, Kengmo-Tchoupa A, Smith SI, Mueller S, Haas R (2016) *Helicobacter pylori* exploits human CEACAMs via HopQ for adherence and translocation of CagA. Nat Microbiol 2(1):1–12. https://doi.org/10.1038/nmicrobiol.2016.188
Kuespert K, Roth A, Hauck CR (2011) *Neisseria meningitidis* has two independent modes of recognizing its human receptor CEACAM1. PLoS ONE 6(1):e14609. https://doi.org/10.1371/journal.pone.0014609
Laskowski RA, MacArthur MW, Thornton JM (1998) Validation of protein models derived from experiment. Curr Opin Struct Biol 8(5):631–639. https://doi.org/10.1016/S0959-440X(98)80156-5
Lázaro-Díez M, Navascués-Lejarza T, Remuzgo-Martínez S, Navas J, Icardo JM, Acosta F, Ramos-Vivas J (2016) Acinetobacter baumannii and A. pittii clinical isolates lack adherence and cytotoxicity to lung epithelial cells in vitro. Microbes Infect 18(9):559–564
Loehfelm TW, Luke NR, Campagnari AA (2008) Identification and characterization of an *Acinetobacter baumannii* biofilm-associated protein. J Bacteriol 190(3):1036–1044. https://doi.org/10.1128/jb.01416-07
Lüthy R, Bowie JU, Eisenberg D (1992) Assessment of protein models with three-dimensional profiles. Nature 356(6364):83–85. https://doi.org/10.1038/356083a0
Maure A, Robino E, Van der Henst C (2023) The intracellular life of *Acinetobacter baumannii*. Trends Microbiol. https://doi.org/10.1016/j.tim.2023.06.007
Mix AK, Goob G, Sontowski E, Hauck CR (2021) Microscale communication between bacterial pathogens and the host epithelium. Genes Immun 22(5–6):247–254. https://doi.org/10.1038/s41435-021-00149-1
Morris FC, Dexter C, Kostoulias X, Uddin MI, Peleg AY (2019) The mechanisms of disease caused by *Acinetobacter baumannii*. Front Microbiol 10:1601. https://doi.org/10.3389/fmicb.2019.01601
Najjar SM (2002) Regulation of insulin action by CEACAM1. Trends Endocrinol Metabolism 13(6):240–245. https://doi.org/10.1016/S1043-2760(02)00608-2
Öbrink B (1997) CEA adhesion molecules: multifunctional proteins with signal-regulatory properties. Curr Opin Cell Biol 9(5):616–626. https://doi.org/10.1016/S0955-0674(97)80114-7
Rangel A, Steenbergen SM, Vimr ER (2016) Unexpected diversity of Escherichia coli sialate O-acetyl esterase NanS. J Bacteriol 198(20):2803–2809. https://doi.org/10.1128/jb.00189-16
Ribet D, Cossart P (2010) Pathogen-mediated posttranslational modifications: a re-emerging field. Cell 143(5):694–702
Sheikh A, Fleckenstein JM (2023) Interactions of pathogenic Escherichia coli with CEACAMs. Front Immunol 14:1120331. https://doi.org/10.3389/fimmu.2023.1120331
Singer BB, Scheffrahn I, Heymann R, Sigmundsson K, Kammerer R, Öbrink B (2002) Carcinoembryonic antigen-related cell adhesion molecule 1 expression and signaling in human, mouse, and rat leukocytes: evidence for replacement of the short cytoplasmic domain isoform by glycosylphosphatidylinositol-linked proteins in human leukocytes. J Immunol 168(10):5139–5146. https://doi.org/10.4049/jimmunol.168.10.5139
van Sorge NM, Bonsor DA, Deng L, Lindahl E, Schmitt V, Lyndin M, Schmidt A, Nilsson OR, Brizuela J, Boero E, Sundberg EJ (2021) Bacterial protein domains with a novel Ig-like Fold target human CEACAM receptors. EMBO J 40(7):106103. https://doi.org/10.15252/embj.2020106103
Viale AM, Evans BA (2020) Microevolution in the major outer membrane protein OmpA of *Acinetobacter baumannii*. Microb Genomics 6(6). https://doi.org/10.1099/mgen.0.000381
Villullas S, Hill DJ, Sessions RB, Rea J, Virji M (2007) Mutational analysis of human CEACAM1: the potential of receptor polymorphism in increasing host susceptibility to bacterial infection. Cell Microbiol 9(2):329–346. https://doi.org/10.1111/j.1462-5822.2006.00789.x
Wollacott AM, Zanghellini A, Murphy P, Baker D (2007) Prediction of structures of multidomain proteins from structures of the individual domains. Protein Sci 16(2):165–175. http://www.proteinscience.org/cgi/doi/10.1110/ps.062270707
Wong D, Nielsen TB, Bonomo RA, Pantapalangkoor P, Luna B, Spellberg B (2017) Clinical and pathophysiological overview of Acinetobacter infections: a century of challenges. Clin Microbiol Rev 30(1):409–447. https://doi.org/10.1111/j.1462-5822.2006.00789.x
Yousef F, Espinosa-Urgel M (2007) Silico analysis of large microbial surface proteins. Res Microbiol 158(6):545–550. https://doi.org/10.1016/j.resmic.2007.04.006
Zilberberg MD, Kollef MH, Shorr AF (2016) Secular trends *in Acinetobacter baumannii* resistance in respiratory and blood stream specimens in the United States, 2003 to 2012: a survey study. J Hosp Med 11(1):21–26. https://doi.org/10.1002/jhm.2477